Phonon superradiance with time delays from collective giant atoms

Ao-Lin Guo,[1,2] Le-Tian Zhu,[2,3] Guang-Can Guo,[2,4] Zhi-Rong Lin,[5,*] Chuan-Feng Li,[2,4,†] and Tao Tu[2,4,‡]

[1]*Department of Basic Course, Space Engineering University, Beijing 101416, China*

[2]*Key Laboratory of Quantum Information, University of Science and Technology of China, Chinese Academy of Sciences, Hefei 230026, People's Republic of China*

[3]*Department of Physics and Astronomy, University of California at Los Angeles, California 90095, USA*

[4]*Hefei National Laboratory, University of Science and Technology of China, Hefei 230088, Peoples Republic of China*

[5]*Shanghai Institute of Microsystem and Information Technology, Shanghai 200050, People's Republic of China*

(Received 19 June 2023; accepted 26 February 2024; published 14 March 2024)

The giant atom regime where the wavelength of the phonon field is smaller than the atomic size opens up new opportunities for exploring exotic phenomena and developing powerful quantum technologies. Here, we explore the radiation dynamics of a hybrid system consisting of a superconducting giant atomic ensemble and an acoustic waveguide. In particular, we show how to design the delayed feedback of the slow acoustic field on the giant atomic ensemble. This modulates the phonon superradiant dynamics into engineerable revival modes and unconventional scaling laws with respect to the number of giant atoms. These are a distinctive feature of time-delayed collective processes that have no analog in other settings. The recipes we provide for harnessing collective giant atoms can be exported to other platforms, laying the foundation for a variety of quantum simulations and applications.

DOI: 10.1103/PhysRevA.109.033711

I. INTRODUCTION

The exploration and design of field-matter interactions is a central component in both fundamental quantum physics and powerful quantum technologies, including rich quantum optical phenomena and quantum simulations, distributed quantum information processing, and quantum networks [1–5]. Studies of the interaction of optical fields and matter have typically focused on the regime where the wavelength of the field is several orders of magnitude larger than the atomic size. Recently, impressive breakthroughs have been made in the coupling of superconducting artificial atoms and acoustic fields [6–12]. The properties of the acoustic field offer the unique opportunity to explore regimes that are not accessible to the optical field. In particular, because of the slower speed of acoustic waves, it is possible to access the vastly different "giant atom" regime where atoms interact with fields whose wavelengths are shorter than the atomic size [13–24]. In this case, the field has a coherent delayed feedback to the atoms, changing the system dynamics with no analog in conventional atom-field systems.

Superradiance is a paradigmatic collective effect where radiation is amplified by the coherence of multiple emitters. This cooperative effect when optical fields and atoms interact have been extensively studied and experimentally observed in a range of physical systems [25–34]. Exploring the interesting interplay of two important processes, the giant atom and collective radiation, will allow relevant quantum simulations and applications to show their full power. However, this new regime has not been explored in the context of field-matter interactions.

In this article, we design a hybrid system consisting of an ensemble of superconducting giant atoms and an acoustic waveguide that can be harnessed to generate and observe time-delayed collective dynamics induced by phonons. The collective effect of the giant atomic ensemble enhances the radiative decay of these emitters, leading to the superradiance of phonons. More interestingly, due to the slow propagation of phonons, the giant emitters are effectively coupled to several acoustic field positions. In contrast to the usual Dicke superradiance of the optical field, this delayed coupling modifies the features of the system dynamics and leads to unconventional collective atom-field interactions and unconventional phonon emission patterns. Since the delay time is customizable, unexplored parameter regimes in field-matter interactions can be realized and characterized. Furthermore, this time-delayed collective behavior establishes a controlled information backflow between the two subsystems, phonons and giant atoms, and thus has potential applications in the quantum information processing based on hybrid systems.

II. SETUP AND MODELS

We propose a tunable hybrid system composed of superconducting giant atoms and a phononic waveguide. As shown in Fig. 1, the giant atomic ensemble is realized by a number of superconducting transmon qubits connected in parallel and coupled to two points of a waveguide via capacitances. For clarity, we consider two coupling points here since wiring

*zrlin@mail.sim.ac.cn
†cfli@ustc.edu.cn
‡tutao@ustc.edu.cn

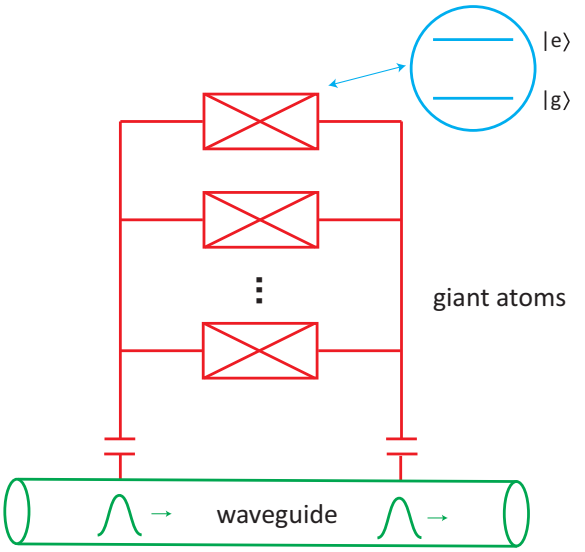

FIG. 1. Schematic of the hybrid setup. A superconducting giant atomic ensemble is coupled to two points x_m, x_{m+1} of a phononic waveguide via capacitances. The superconducting artificial atoms and phonon fields can be controlled and detected by the external gates. The time-delayed nature of the system arises from the interference in the nonlocal points.

up to multiple coupling points becomes complicated. The phononic waveguide is constructed by propagating surface acoustic waves on a piezoelectric substrate. This hybrid system has a wide range of tunable parameters, including driving atomic ensembles and detecting phonon fields by the external gates. All elements of our proposal can be implemented in the current experimental setups [35–38]. The Hamiltonian of this hybrid system is

$$H = \sum_{i=1}^{N} \frac{\Omega_i}{2}\sigma_{iz} + \int \omega_k a_k^+ a_k dk + \sum_{m=1}^{2} \int g_0 \times \left(e^{ikx_m} a_k \sum_{i=1}^{N} \sigma_{i+} + e^{-ikx_m} a_k^+ \sum_{i=1}^{N} \sigma_{i-}\right) dk. \quad (1)$$

Here σ is the Pauli operator of the superconducting qubit and a^+ and a are the creation and annihilation operators of the phonon field. The subscript i denotes the qubit while the subscript m labels the coupling point of the atomic ensemble to the waveguide. The parameter Ω is the transition frequency of the qubit and ω_k and k are the frequency and wave vector of the phonon mode. The propagation time of the phonon field between two adjacent points is $\tau_d = (x_{m+1} - x_m)/v$, where v is the wave velocity of sound. Thus the interaction of the giant atomic ensemble and the phonon field has a delay time τ_d. This characteristic time leads to interference between the nonlocal coupling points, which brings substantial changes in the system dynamics. For a detailed derivation of this Hamiltonian, see the Appendix A.

III. SUPERRADIANCE OF PHONONS

First we consider the usual case of small atoms. When the wave speed is very large, for a given frequency the wavelength of phonon field is much larger than the size of the superconducting circuit. In this case, the hybrid system is approximated as the interaction of N artifical atoms and a single-mode field

$$H_0 = \sum_i \frac{\Omega_i}{2}\sigma_{iz} + \omega_r a^+ a + g_0\left(a\sum_i \sigma_{i+} + a^+ \sum_i \sigma_{i-}\right). \quad (2)$$

To explore this hybrid system, we apply a pulse to drive the superconducting artificial atoms. Initially the atomic ensemble is in the ground state and by the driving pulse the atomic ensemble achieves an inversion. Due to the coupling of the atomic ensemble to the phonon field, the atomic excited state is transferred to the phonon mode, which manifests itself as phonon radiation.

Since phonon radiation is the result of the collective decay of artificial atoms, it is of interest to study the dynamics of the system operators during this process. For an ensemble of artificial atoms, we can make two approximations as follows. First, the atoms have the same transition frequency. Second, the coupling strengths of the atoms and phonon fields are also the same. Thus the ensemble can be described by a collective atom operator $S = \sum_i \sigma_i$.

However, relaxation and dephasing affect the coherence of the atomic ensemble and thus reduce the intensity of phonon radiation. To account for these decoherence processes, we use the master equation

$$\frac{d\rho}{dt} = -\frac{i}{\hbar}[H_0, \rho] + \kappa L[a] + \gamma_1 \sum_i L[\sigma_{i-}] + \gamma_\phi \sum_i L[\sigma_{iz}]. \quad (3)$$

Here ρ is the density matrix of the system, L is the Lindblad operator $L[O] = O\rho O - 1/2(O^+O\rho - \rho O^+O)$, and κ, γ_1, γ_ϕ are the leakage rate of the phononic waveguide, the relaxation rate, and the dephasing rate of the atoms, respectively.

From this model, we can derive the equations of motion for the expectation value of system operators

$$\begin{aligned}
\frac{d\langle S_z\rangle}{dt} &= -2ig_0(\langle a\rangle\langle S_-\rangle^* - \langle a\rangle^*\langle S_-\rangle) - \gamma_1(\langle S_z\rangle + N),\\
\frac{d\langle S_-\rangle}{dt} &= ig_0\langle a\rangle\langle S_z\rangle - \left(\frac{\gamma_1}{2} + \gamma_\phi + i\Delta\right)\langle S_-\rangle,\\
\frac{d\langle a\rangle}{dt} &= -ig_0\langle S_-\rangle - \left(\frac{\kappa}{2} + i\delta\right)\langle a\rangle. \quad (4)
\end{aligned}$$

Here we use the rotating frame as $\Delta = \Omega - \omega$ and $\delta = \omega_r - \omega$, as well as the mean-field approximation, e.g., $\langle aS_z\rangle \approx \langle a\rangle\langle S_z\rangle$. This approximation is valid because there are a large number of atoms in the ensemble and their fluctuations can be neglected [39–43]. We use Eq. (4) to simulate the dynamics of the hybrid system in the small atom regime. The parameters in the simulation use the actual values extracted from the experiments [18–21].

In Fig. 2(a), we give the simulation results for the emitted phonons from the atomic ensemble. After the driving pulse, the ensemble reaches an inversion and stays in this highly polarized state for some time. Then the atoms decay due to the stimulation of thermal and vacuum fluctuations. Along with the collective decay of atoms, a burst of phonons is emitted into the waveguide, which is the characteristic burst of phonon superradiance. Here we use a typical dephasing time

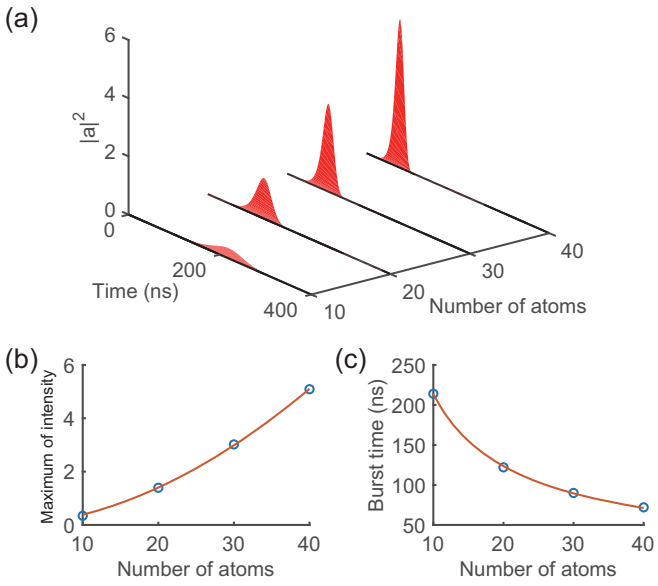

FIG. 2. Phonon superradiance in the small atom regime. (a) Time trace of phonon radiation for different numbers N of atoms in the ensemble. (b), (c) The maximum value and the burst time of phonon radiation as functions of N. The parameters are the coupling strength $g_0 = 20\,\mathrm{MHz}$, waveguide leakage $\kappa = 0.3\,\mathrm{GHz}$, atomic relaxation and dephasing rates $\gamma_1 = 0.145\,\mathrm{MHz}$, $\gamma_\phi = 0.125\,\mathrm{MHz}$.

of superconducting qubits, which is comparable to the burst time of phonons. The dissipation effects play a significant role in the collective process of atoms, which reduces the intensity of phonon superradiance.

Further, we study the scaling behavior of phonon superradiance. In Fig. 2(a), we show the dynamics of phonon radiation for different numbers N of atoms in the ensemble. From the figure we find that the maximum intensity and the peak time of the phonon burst change as the number of atoms increases. In Figs. 2(b) and 2(c), we can fit the height and time of the phonon burst as a function of N. This scaling law with respect to the atom number clearly shows the collective nature of phonon emission from atomic ensembles.

The above phonon superradiance can be analyzed in a simple case to obtain an intuitive physical picture. In the fast waveguide limit, we can derive an effective equation of motion of the atomic ensemble

$$\frac{d\langle S_z\rangle}{dt} = -\frac{8g_0^2}{\kappa}\langle S_+S_-\rangle - \gamma_1(\langle S_z\rangle + N). \tag{5}$$

The first term shows that the dynamics of the ensemble polarization $\langle S_z\rangle$ depends on the coherence of the ensemble $\langle S_+S_-\rangle$. The coefficient of this term is the usual Purcell factor $4g_0^2/\kappa$, which is the decay rate of a single atom through the phonon emission channel. Since the coherence of the ensemble is proportional to the number of atoms in the ensemble $\langle S_+S_-\rangle \sim N^2$, its decay rate, and the corresponding phonon emission rate are greatly enhanced compared to the case of a single atom. Figure 2(a) clearly shows this enhancement due to the collective effect of atoms in the ensemble.

This effective equation of motion also accounts for the behavior of the scaling law. Ideally, the coherence of the ensemble in Eq. (5) is proportional to N^2. However, other dissipation channels exist, such as the second term in Eq. (5). The competition between different decay channels leads to a deviation of the phonon radiation from the scaling law of N^2, showing a smaller scaling law. For the derivation of the effective equation and the analysis of various dissipative effects, see Appendixes B and C, respectively. The enhanced radiation and scaling laws due to collective effects are consistent with the expectations of the effective equation of motion and are indicators of phonon superradiance.

IV. COLLECTIVE RADIATION WITH TIME DELAYS

When the speed of acoustic waves is slow, it is possible to access the giant atom regime. The propagation time τ_d of phonons between two adjacent points can be much larger than the decay time of the giant atomic ensemble. In this case, the phonons emitted to the waveguide at one coupling point due to giant atoms may later be reabsorbed at a second coupling point. Thus, starting from the complete Hamiltonian Eq. (1) we derive its equations of motion as

$$\begin{aligned}
\frac{d\langle S_z\rangle}{dt} &= -2ig_0\sum_{m=1}^{2}\int (e^{ikx_m}\langle a_k\rangle\langle S_-\rangle^* \\
&\quad - e^{-ikx_m}\langle a_k\rangle^*\langle S_-\rangle)\sqrt{|k|}dk - \gamma_1(\langle S_z\rangle + N), \\
\frac{d\langle S_-\rangle}{dt} &= ig_0\langle S_z\rangle\sum_{m=1}^{2}\int e^{ikx_m}\langle a_k\rangle\sqrt{|k|}dk \\
&\quad - \left(\frac{\gamma_1}{2} + \gamma_\phi + i\Delta\right)\langle S_-\rangle, \\
\frac{d\langle a_k\rangle}{dt} &= -ig_0\langle S_-\rangle\sqrt{|k|}\sum_{m=1}^{2}e^{-ikx_m} - \left(\frac{\kappa}{2} + i\delta_k\right)\langle a_k\rangle.
\end{aligned} \tag{6}$$

We use Eq. (6) to model the dynamics of the hybrid system in the giant atom regime.

Before the numerical simulation of Eq. (6), to represent the effect of slow phonons more clearly, we derive an effective equation for the evolution of $\langle S_-\rangle$,

$$\begin{aligned}
\frac{d\langle S_-\rangle}{dt} &= i\Delta\langle S_-\rangle - \gamma_m\langle S_z\rangle\langle S_-\rangle - \left(\frac{\gamma_1}{2} + \gamma_\phi\right)\langle S_-\rangle \\
&\quad - \gamma_m\langle S_z\rangle\langle S_-\rangle(t-\tau_d)\Theta(t-\tau_d).
\end{aligned} \tag{7}$$

Here $\gamma_m = 4\pi(\frac{g_0}{v})^2\Omega$ is the phonon emission rate at a single coupling point. the first term describes the coherent evolution of the atomic ensemble, the second term describes the relaxation process in the environment, and the third term describes the process of emitting phonons from the atomic ensemble. The last term contains a Heaviside function Θ that describes the delayed feedback on the atomic ensemble at time τ_d due to the slow propagation of the phonon field. In contrast to the case where the delay time τ_d is not considered, the dynamics of the giant atomic ensemble as in Eq. (7) clearly introduces a delayed coupling term. For a detailed derivation of these equations see Appendix C.

First we study the system behavior in the time domain. In Figs. 3(a) and 3(b) we show the simulation results of phonon radiation and giant atomic ensemble polarization, respectively. The dynamics of phonon superradiance exhibits a

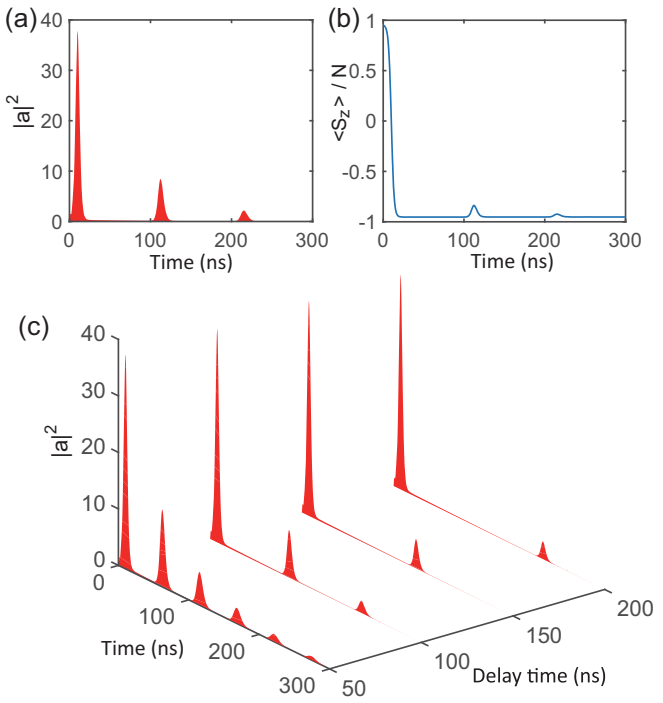

FIG. 3. Dynamics of time-delayed phonon superradiance. (a, b) Time evolution of the phonon radiation and the polarization of the giant atomic ensemble. (c) Intensity of phonon radiation of giant atom ensembles as a function of evolution time and delay time. The parameters are the number of giant atoms $N = 20$, coupling strength $g_0 = 50\,\mathrm{MHz}$, waveguide leakage $\kappa = 10\,\mathrm{MHz}$, delay time $\tau_d = 100\,\mathrm{ns}$, and other parameters are the same as in Fig. 2.

multipeak structure, which is very different from the usual single-peak structure in the case of small atoms with $\tau_d = 0$ (Fig. 2). The first radiation burst is followed by a series of smaller ones. The polarization of the giant atomic ensemble corresponds one-to-one to the phonon emission, and both have the same feature: the time spacing of the peaks is τ_d. The accumulated phase of the phonons during their propagation between the two coupling points induces the interference effects that produce these peaks.

Since the introduced delay time is deterministic, we can design this hybrid system. In Fig. 3(c), we show the simulation results for phonon radiation with different delay times. We find that the revival peaks after the first radiation burst appear sequentially at integer multiples of the delay time τ_d. In the present case, the giant atom subsystem and the phonon subsystem have a structured coupling. The phonon field acquires a longer memory time than the decay time of the giant atomic ensemble, producing a delayed feedback to the atomic ensemble. This manifests itself as a revival in the time trajectory.

The study of the scaling behavior of the collective radiation in the giant-atom regime can bring additional insight. In Fig. 4, we show the scaling behavior of the maximum intensity of the second phonon peak with respect to the number of giant atoms N in the ensemble at different delay times. The scaling law of the phonon superradiance changes significantly with the delay time. This is because as the delay time increases,

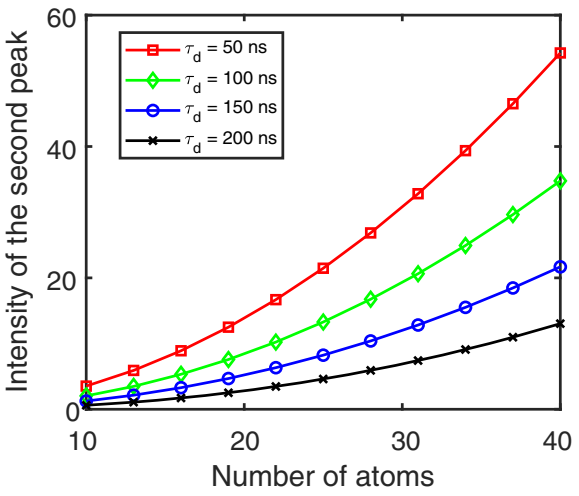

FIG. 4. Scaling laws for non-Markovian phonon superradiance. The phonon field intensity of the second peak are displayed as a function of giant atoms in the ensemble at different delay times. The parameters are the same as in Fig. 3.

the phonon radiation peak appears later, leading to a decrease in its intensity due to dissipation effects. For the combined effects of various dissipation times and delay times, see Appendix D.

V. DISCUSSION AND CONCLUSION

To realize our scheme in a realistic device, we analyze the effect of disorder in the atomic energies and in the atom-waveguide couplings.

First, in the equation of motion for our system, there is a collective emission term $\frac{g_0^2}{\kappa}\langle S_+ S_-\rangle$. It is this term that induces superradiant emission, as given by the radiation intensity $I \sim N\frac{g_0^2}{\kappa}$. Here N is the number of excitations in the atomic ensemble, g_0 is the atom-waveguide coupling strength, and κ is the decay rate of the waveguide. One can expect to observe such superradiance phenomena when the emission rate is larger than the inhomogeneities $\delta\Omega$, δg_0 in the atomic energies and atom-waveguide couplings. In practice, as the number of superconducting qubits increases, one can observe superradiance even with large values of inhomogeneity. For example, using realistic parameters in current experiments [35–38], $N = 20$, $g_0 = 50\,\mathrm{MHz}$, $\kappa = 10\,\mathrm{MHz}$, $\delta\Omega = 0.2\,\mathrm{MHz}$, $\delta g_0 = 1\,\mathrm{MHz}$, we can find that the value of emission rate $N\frac{g_0^2}{\kappa}$ is much larger than that of the inhomogeneities $\delta\Omega$, δg_0 in the atomic energies and atom-waveguide couplings.

Second, the dephasing time of the atomic system is dominated by the inhomogeneity $\delta\Omega$ of the atomic energies. We can assess the effect of the dephasing time of giant atoms on the superradiance behavior. As detailed in Appendix D, the simulation results indicate that the atomic dephasing time has a slight effect on the phonon superradiance.

Finally, one of obstacle of applications of an ensemble of superconducting qubits is the inhomogeneity of atomic energies. As pointed out in Ref. [41], the inhomogeneity of superconducting qubits can be effectively suppressed by applying an external magnetic flux.

In summary, we propose a method to engineer effective delayed field-matter couplings using superconducting giant atomic ensembles and acoustic waveguides. We also illustrate that this implementation yields unconventional collective quantum phononic behavior. In particular, exotic phonon emission patterns and collective atomic interactions are obtained, such as the decay-recovery structure of the system dynamics. These methods can be applied to other hybrid platforms, offering a flexibility to interact coherently with different quantum systems [44–46]. In addition to the fundamental interest of these phenomena, there are many possible applications. In quantum simulations, the setup provides a flexible platform for probing nonequilibrium many-body physics [47–49]. In addition, one can exploit the tunability of phonon feedback to encode quantum information into decoherence free subspaces or into cluster states, which can be used for fault-tolerant quantum computing [16,50,51]. This controlled collective radiation effect also enables highly sensitive phonon-based measurements and narrow bandwidth phonon radiation [52–54].

ACKNOWLEDGMENTS

This work was supported by the National Natural Science Foundation of China (Grant No. 11974336) and Innovation Program for Quantum Science and Technology (Grant No. 2021ZD0301200).

APPENDIX A: TOTAL HAMILTONIAN OF THE HYBRID SYSTEM

We give detailed derivations of the Hamiltonian (1) used in the main text. When multiple superconducting transmon qubits are coupled to a phonon waveguide via capacitances, the total Hamiltonian of the hybrid system is given by [37]

$$\begin{aligned} H_t &= \sum_i \frac{(2e)^2}{2C_t}(\hat{n}_i - \hat{n}_s)^2 - \sum_i E_J \cos\hat{\varphi}_i \\ &= \sum_i \left(4E_C\hat{n}_i^2 - E_J\cos\hat{\varphi}_i - 8E_C\hat{n}_i\hat{n}_s + 4E_C\hat{n}_s^2\right). \end{aligned} \tag{A1}$$

On the one hand, $\hat{n}_i$ is the charge number operator of the ith transmon qubit, $\hat{n}_s$ is the offset charge, both measured in units of the Cooper pair charge $2e$, $E_C = e^2/2C_t$ is the charging energy, and C_t is the total capacitance of the transmon qubit. On the other hand, $\hat{\varphi}_i$ is the phase operator of the ith transmon qubit and E_J is the Josephson energy.

We introduce the Pauli operators σ_- and σ_+ of the transmon qubit via $\hat{\varphi} = \sqrt{\frac{\eta}{2}}(\sigma_- + \sigma_+)$ and $\hat{n} = -i\sqrt{\frac{1}{2\eta}}(\sigma_- - \sigma_+)$ with $\eta = \sqrt{8E_C/E_J}$. Therefore, the Hamiltonian of the superconducting artificial atomic ensemble can be expressed as

$$\begin{aligned} H_{qs} &= \sum_i \left(4E_C\hat{n}_i^2 - E_J\cos\varphi_i\right) \\ &\approx \sum_i \hbar\omega_0\left(\sigma_{i+}\sigma_{i-} + \frac{1}{2}\right) - \sum_i \chi(\sigma_{i-} + \sigma_{i+})^4, \end{aligned} \tag{A2}$$

where $\omega_0 = \sqrt{8E_CE_J}/\hbar$ is the transition frequency of the transmon qubit and $\chi = E_C/12$ is the nonlinear term.

The electric potential field $\xi(x,t)$ in the phonon waveguide is described by

$$\xi(x,t) = -i\sqrt{\frac{\hbar Z_0 v}{4\pi}}\int_{-\infty}^{\infty} dk\sqrt{\omega_k}(\hat{a}_k e^{-i(\omega_k t - kx)} - \text{H.c.}). \tag{A3}$$

Here $\hat{a}_k$ is the annihilation operator of the phonon mode with wave vector k, Z_0 is the characteristic impedance of the phonon waveguide, v is the velocity of surface acoustic wave (SAW) phonons, which satisfies the dispersion relation $\omega_k = |k|v$.

In Eq. (A1), the interaction between the superconducting artificial atomic ensemble and the phonon waveguide is described by the following term $H_{\text{int}} = \sum_i -8E_C\hat{n}_i\hat{n}_s$. The offset charge is $\hat{n}_s = (2e)^{-1}\sum_{m=1}^{2} C_g\xi(x_m,t)$ where C_g and x_m are the coupling capacitance and position of each coupling point, respectively [7,18,19]. Thus, we can calculate the interaction Hamiltonian as follows:

$$\begin{aligned} H_{\text{int}} &= \sum_{j=1}^{N} -8E_C\hat{n}_j\hat{n}_s \\ &= \sum_{j=1}^{N} -i8E_C\sqrt{\frac{1}{2\eta}}(\sigma_{j-} - \sigma_{j+})\frac{1}{2e}\sum_{m=1}^{2} C_g\xi(x_m,t) \\ &= \frac{4E_C}{e}\sqrt{\frac{1}{2\eta}}\sqrt{\frac{\hbar Z_0 v}{4\pi}} \times \sum_{j=1}^{N}\sum_{m=1}^{2} C_g\int_{-\infty}^{\infty} dk\sqrt{\omega_k} \\ &\quad \times(a_k e^{ikx_m} - \text{H.c.})(\sigma_{j-} - \sigma_{j+}) \\ &\approx \sum_{j=1}^{N}\sum_{m=1}^{2}\int_{-\infty}^{\infty} g_0(a_k\sigma_{j+}e^{ikx_m} + \text{H.c.})\sqrt{|k|}dk. \end{aligned} \tag{A4}$$

In the above derivation, we use the rotating-wave approximation (RWA) to neglect the counterrotating terms $a_k^\dagger\sigma_+$ and $a_k\sigma_-$. In addition, we define the coupling strength $g_0 = \frac{4E_C}{e}\sqrt{\frac{1}{2\eta}}\sqrt{\frac{\hbar Z_0}{4\pi}}vC_g$ and use the linear dispersion relation $\omega_k = v|k|$.

Putting things together, we obtain the total Hamiltonian in the main text as

$$\begin{aligned} H &= \sum_{i=1}^{N}\frac{\Omega_i}{2}\sigma_{iz} + \int \omega_k a_k^+ a_k dk \\ &\quad + \sum_{m=1}^{2}\int g_0\left(e^{ikx_m}a_k\sum_i\sigma_{i+} + e^{-ikx_m}a_k^+\sum_i\sigma_{i-}\right)dk. \end{aligned} \tag{A5}$$

APPENDIX B: THEORY OF PHONON SUPERRADIANCE IN THE SMALL ATOM REGIME

We present detailed derivations of Eqs. (2) to (5) used in the main text.

1. Hamiltonian

We begin with the usual case of small atoms. When the velocity of SAWs is very large, for a given frequency the wavelength of phonon field is much larger than the size of

the superconducting circuit. In this case, the hybrid system is described by a Tavis-Cumming Hamiltonian with N artificial atoms coupled to a single-mode phonon field [39–43]

$$H_0 = \sum_i \frac{\Omega_i}{2}\sigma_{iz} + \omega_r a^+ a + g_0\left(a\sum_i \sigma_{i+} + a^+\sum_i \sigma_{i-}\right). \tag{B1}$$

In a rotating frame with frequency ω, the above Hamiltonian is given by

$$H_0 = \sum_i \frac{\Delta_i}{2}\sigma_{iz} + \delta a^+ a + g_0\left(a\sum_i \sigma_{i+} + a^+\sum_i \sigma_{i-}\right), \tag{B2}$$

where the detunings are $\Delta = \Omega - \omega$ and $\delta = \omega_r - \omega$, respectively.

2. Equations of motion

Relaxation and dephasing will significantly affect the coherence of the atomic ensemble. In the presence of dissipation, the dynamics of the hybrid system is described by the master equation

$$\frac{d\rho}{dt} = -i[H_0, \rho] + \gamma_1 \sum_i L[\sigma_{i-}] + \frac{\gamma_\phi}{2}\sum_i L[\sigma_{iz}] + \kappa L[a], \tag{B3}$$

where the dissipation effects are included in the Lindblad term $L[O] = O\rho O^+ - 1/2(O^+O\rho - \rho O^+O)$ and κ, γ_1, γ_ϕ are the leakage rate of the acoustic waveguide, the relaxation rate and the dephasing rate of the atoms, respectively.

We use the collective spin operator to describe the atomic ensemble, which is defined as $S_{(z,+,-)} = \sum_i \sigma_{i(z,+,-)}$. From the master equation, we can derive the equation of motion for the expectation value of the system operator as follows [55]:

$$\begin{aligned}\frac{d\langle S_z\rangle}{dt} &= -i\langle[S_z, H_0]\rangle - \gamma_1(N + \langle S_z\rangle \\ &= -i2g_0(\langle aS_+\rangle - \langle a^+S_-\rangle) - \gamma_1(N + \langle S_z\rangle),\end{aligned} \tag{B4}$$

$$\begin{aligned}\frac{d\langle S_-\rangle}{dt} &= -i\langle[S_-, H_0]\rangle - \left(\frac{\gamma_1}{2} + \gamma_\phi\right)\langle S_-\rangle \\ &= -i\Delta\langle S_-\rangle + ig_0\langle aS_z\rangle - \left(\frac{\gamma_1}{2} + \gamma_\phi\right)\langle S_-\rangle,\end{aligned} \tag{B5}$$

$$\frac{d\langle a\rangle}{dt} = -i\langle[a, H_0]\rangle - \frac{\kappa}{2}\langle a\rangle = -i\delta\langle a\rangle - ig_0\langle S_-\rangle - \frac{\kappa}{2}\langle a\rangle. \tag{B6}$$

3. Effective equation of motion and scaling behaviors

We now consider the fast waveguide limit. Since the dynamic timescale of the waveguide is much faster than that of the atomic ensemble, we can assume that $\frac{d\langle a\rangle}{dt} = 0$, which gives the steady-state solution for the phonon field amplitude $\langle a\rangle$. We substitute this expression back into the above equations to obtain the effective equation of motion for the atomic collective operator

$$\frac{d\langle S_z\rangle}{dt} = -\frac{8g_0^2}{\kappa}\langle S_+S_-\rangle - \gamma_1(N + \langle S_z\rangle). \tag{B7}$$

Note that the coherence term of the atomic ensemble can be expressed as $\langle S_+S_-\rangle = \sum_i\langle\sigma_{i+}\sigma_{i-}\rangle + \sum_{i,j}\langle\sigma_{i+}\sigma_{j-}\rangle$. The first term is the number of polarizations, proportional to the number of atoms N in the ensemble. The second term is the interference between different atoms, which contains N^2 elements and leads to a scaling law of the phonon superradiance. Since there are other decoherence processes, in realistic cases the exponent of the scaling law is a value smaller than 2.

APPENDIX C: THEORY OF PHONON SUPERRADIANCE IN THE GIANT ATOM REGIME

We present detailed derivations of Eqs. (6) and (7) used in the main text.

1. Hamiltonian

By defining the collective spin operator S, the total Hamiltonian Eq. (A5) is written as

$$\begin{aligned}H = &\frac{\Omega}{2}S_z + \int \omega_k a_k^+ a_k dk \\ &+ \sum_{m=1}^{2}\int g_0(e^{ikx_m}a_k S_+ + e^{-ikx_m}a_k^+ S_-)\sqrt{|k|}dk.\end{aligned} \tag{C1}$$

2. Equations of motion

In the presence of environmental dissipations, the dynamics of the hybrid system is described by the master equation

$$\frac{d\rho}{dt} = -i[H, \rho] + \gamma_1 L[S_-] + \frac{\gamma_\phi}{2}L[S_z] + \kappa L[a], \tag{C2}$$

where the dissipation effects are included in the Lindblad term, and κ, γ_1, γ_ϕ are the waveguide leakage rate, the atomic relaxation rate, and dephasing rate, respectively.

Starting from the above master equation, we can obtain the equations of motion for the giant atomic ensemble and the phonon field [55]

$$\begin{aligned}\frac{d\langle S_z\rangle}{dt} &= -i\langle[S_z, H]\rangle - \gamma_1(N + \langle S_z\rangle \\ &= -2ig_0\sum_{m=1}^{2}\int (e^{ikx_m}\langle a_k\rangle\langle S_-\rangle^* \\ &\quad - e^{-ikx_m}\langle a_k\rangle^*\langle S_-\rangle)\sqrt{|k|}dk - \gamma_1(\langle S_z\rangle + N),\end{aligned} \tag{C3}$$

$$\begin{aligned}\frac{d\langle S_-\rangle}{dt} &= -i\langle[S_-, H]\rangle - \left(\frac{\gamma_1}{2} + \gamma_\phi\right)\langle S_-\rangle \\ &= ig_0\langle S_z\rangle\sum_{m=1}^{2}\int e^{ikx_m}\langle a_k\rangle\sqrt{|k|}dk \\ &\quad - \left(\frac{\gamma_1}{2} + \gamma_\phi + i\Delta\right)\langle S_-\rangle,\end{aligned} \tag{C4}$$

$$\frac{d\langle a_k\rangle}{dt} = -i\langle[a,H]\rangle - \frac{\kappa}{2}\langle a\rangle = -ig_0\langle S_-\rangle\sqrt{|k|}\sum_{m=1}^{2} e^{-ikx_m} - \left(\frac{\kappa}{2} + i\delta_k\right)\langle a_k\rangle. \tag{C5}$$

3. Effective equation of motion for $\langle S_-\rangle$

During phonon radiation, on the one hand, giant atoms emit phonons, and on the other hand, already emitted phonons are reabsorbed by giant atoms, leading to a delayed feedback of phonons to giant atoms. The above equations of motion are complex, so it is instructive to obtain an effective equation of motion that obviously includes delayed dynamics. For clarity, we neglect the environmental terms in the above euqations first. We use the following steps to dervie the effective equation [15].

Step 1: Obtain a formal solution of the phonon field.

Integrating Eq. (C5), we have the formal solution

$$\langle a_k\rangle(t) = e^{-i\omega_k t}[\langle a_k\rangle(0) - ig_0\sqrt{|k|}\sum_{m=1}^{2} e^{-ikx_m} \times \int_0^t \langle S_-\rangle(t')e^{i\omega_k t'}dt']. \tag{C6}$$

Step 2: Transform the integral of the wave vector k to the integral of the frequency ω.

Substituting the formal solution of the phonon field into Eq. (C4), we have

$$\begin{aligned}
\frac{d\langle S_-\rangle}{dt} &= -i\Omega\langle S_-\rangle + ig_0\langle S_z\rangle\sum_{m=1}^{2}\int_{-\infty}^{+\infty} e^{ikx_m}[e^{-i\omega_k t}(\langle a_k\rangle(0) - ig_0\sqrt{|k|}\sum_{m=1}^{2} e^{-ikx_{m'}}\int_0^t \langle S_-\rangle(t')e^{i\omega_k t'}dt')]\sqrt{|k|}dk \\
&= -i\Omega\langle S_-\rangle + ig_0\langle S_z\rangle\sum_{m=1}^{2}\int_{-\infty}^{+\infty}\sqrt{|k|}e^{ikx_m - i\omega_k t}\langle a_k\rangle(0)dk + (g_0)^2\langle S_z\rangle\sum_{m=1}^{2}\sum_{m'=1}^{2}\int_0^t\langle S_-\rangle(t')dt'\int_{-\infty}^{+\infty}|k|e^{ik(x_m - x_{m'}) + i\omega_k(t'-t)}dk \\
&= -i\Omega\langle S_-\rangle + i\frac{g_0}{\sqrt{v}}\langle S_z\rangle\sum_{m=1}^{2}\int_0^{+\infty}\sqrt{\omega_k}e^{ikx_m - i\omega_k t}\langle a_k\rangle(0)d\omega_k \\
&\quad + \left(\frac{g_0}{v}\right)^2\langle S_z\rangle\sum_{m=1}^{2}\sum_{m'=1}^{2}\int_0^t\langle S_-\rangle(t')dt'\int_0^{+\infty}\omega_k[e^{i\frac{\omega_k}{v}(x_m - x_{m'}) + i\omega_k(t'-t)} + e^{-i\frac{\omega_k}{v}(x_m - x_{m'}) + i\omega_k(t'-t)}]d\omega_k \\
&= -i\Omega\langle S_-\rangle + i\frac{g_0}{\sqrt{v}}\langle S_z\rangle\sum_{m=1}^{2}\int_0^{+\infty}\sqrt{\omega_k}e^{ikx_m - i\omega_k t}\langle a_k\rangle(0)d\omega_k + \left(\frac{g_0}{v}\right)^2\langle S_z\rangle\sum_{m=1}^{2}\sum_{m'=1}^{2}\int_0^t\langle S_-\rangle(t')dt' \\
&\quad \times\int_0^{+\infty}\omega_k[e^{i\omega_k\tau_{mm'} + i\omega_k(t'-t)} + e^{-i\omega_k\tau_{mm'} + i\omega_k(t'-t)}]d\omega_k.
\end{aligned}$$

Here we define the delay time between two coupling points as $\tau_{mm'} = \frac{(x_m - x_{m'})}{v}$.

Step 3: Calculate the integral of the frequency ω.

According to the Weisskopf-Wigner approximation, the radiation is mainly concentrated at the atomic transition frequency Ω. That is, the frequency ω_k of the radiation field is concentrated in a very narrow range around Ω. Thus we can define the integral limit of ω_k as going from negative infinity to positive infinity. Then by using the integral formula $\int_{-\infty}^{+\infty} e^{i\omega_k t}d\omega_k = 2\pi\delta(t)$, we get

$$\begin{aligned}
\frac{d\langle S_-\rangle}{dt} &= -i\Omega\langle S_-\rangle + i\frac{g_0}{\sqrt{v}}\langle S_z\rangle\sum_{m=1}^{2}\int_{-\infty}^{+\infty}\sqrt{\omega_k}e^{ikx_m - i\omega_k t}\langle a_k\rangle(0)d\omega_k + \left(\frac{g_0}{v}\right)^2\langle S_z\rangle\sum_{m=1}^{2}\sum_{m'=1}^{2}\int_0^t\langle S_-\rangle(t')dt' \\
&\quad\times\int_{-\infty}^{+\infty}\omega_k[e^{i\omega_k\tau_{mm'} + i\omega_k(t'-t)} + e^{-i\omega_k\tau_{mm'} + i\omega_k(t'-t)}]d\omega_k = -i\Omega\langle S_-\rangle + i\frac{g_0}{\sqrt{v}}\langle S_z\rangle\sum_{m=1}^{2}\int_{-\infty}^{+\infty}\sqrt{\omega_k}e^{ikx_m - i\omega_k t}\langle a_k\rangle(0)d\omega_k \\
&\quad + \left(\frac{g_0}{v}\right)^2\langle S_z\rangle\sum_{m=1}^{2}\sum_{m'=1}^{2}\int_0^t\langle S_-\rangle(t')dt'\omega_k[2\pi\delta(t'-t+\tau_{mm'}) + 2\pi\delta(t'-t-\tau_{mm'})] \\
&= -i\Omega\langle S_-\rangle + i\frac{g_0}{\sqrt{v}}\langle S_z\rangle\sum_{m=1}^{2}\int_{-\infty}^{+\infty}\sqrt{\omega_k}e^{ikx_m - i\omega_k t}\langle a_k\rangle(0)d\omega_k + \frac{\gamma_m}{2}\langle S_z\rangle\sum_{m=1}^{2}\sum_{m'=1}^{2}\int_0^t\langle S_-\rangle(t')dt' \\
&\quad\times[\delta(t'-t+\tau_{mm'}) + \delta(t'-t-\tau_{mm'})].
\end{aligned}$$

Here we define the radiation rate as $\gamma_m = 4\pi(\frac{g_0}{v})^2\Omega$.

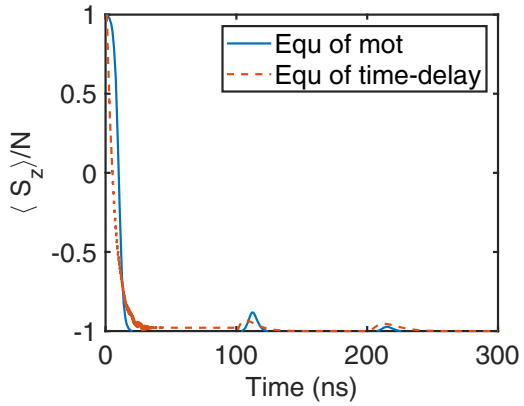

FIG. 5. Time evolution of the polarization of the giant atomic ensemble. The solid line is the simulation result of the equation of motion (6) and the dashed line is the simulation result of the time-delayed Eq. (7). The parameters are the number of giant atoms $N = 20$, coupling strength $g_0 = 50\,\mathrm{MHz}$, waveguide leakage $\kappa = 10\,\mathrm{MHz}$, delay time $\tau_d = 100\,\mathrm{ns}$, and other parameters are the same as in Fig. 2.

Step 4: Calculate the integral over time t.

Now we use the integral formula $\int_0^t \delta(t'-\tau)dt' = \Theta(t-\tau)$ where Θ is the Heaviside step function, so that we obtain

$$\frac{d\langle S_-\rangle}{dt} = -i\Omega\langle S_-\rangle - \gamma_m\langle S_z\rangle\langle S_-\rangle - \gamma_m\langle S_z\rangle\langle S_-\rangle(t-\tau_d)\Theta(t-\tau_d). \tag{C7}$$

Here the second and third terms on the right-hand side clearly show that phonons emitted from the first coupling point are reabsorbed at the second coupling point. In the giant atom regime, the time-delayed coupling term in the effective equation gives rise to unconventional collective dynamics, which is the main result of this paper. Including the dissipation term from the environment, we can obtain the following effective equation of motion

$$\frac{d\langle S_-\rangle}{dt} = i\Omega\langle S_-\rangle - \gamma_m\langle S_z\rangle\langle S_-\rangle - \left(\frac{\gamma_1}{2}+\gamma_\phi\right)\langle S_-\rangle - \gamma_m\langle S_z\rangle\langle S_-\rangle(t-\tau_d)\Theta(t-\tau_d). \tag{C8}$$

4. Effective equation of motion for $\langle S_z\rangle$

In the previous section we present the effective equation for the coherence of the giant atomic ensemble. Here we obtain the effective equation for the polarization of the giant atomic ensemble in a similar way

$$\frac{d\langle S_z\rangle}{dt} = -2\gamma_m\langle S_+\rangle\langle S_-\rangle - \gamma_1(\langle S_z\rangle + N) - \gamma_m\langle S_+\rangle\langle S_-\rangle(t-\tau_d)\Theta(t-\tau_d) - \gamma_m\langle S_-\rangle\langle S_+\rangle(t-\tau_d)\Theta(t-\tau_d). \tag{C9}$$

In addition to the above analytical derivations, we numerically calculate the dynamics of the system using the equation of motion (6) and the effective equation of motion with time delays (7), respectively. As shown in Fig. 5, there are some minor differences between the two calculations in a short period of time, but in a larger time range, the results of both calculations are in good agreement.

APPENDIX D: SIMULATION RESULTS OF PHONON SUPERRADIANCE

1. Dissipation effects on phonon superradiance in the small atom regime

By numerically solving the equations of motion (4) of the hybrid system in the main text, we give the simulation results of its dynamics in the small atom regime. In Fig. 6(a), we show the effect of waveguide leakage processes on phonon radiation. In Fig. 6(b), we show the corresponding dynamics of the polarization of the atomic ensemble. In the slow

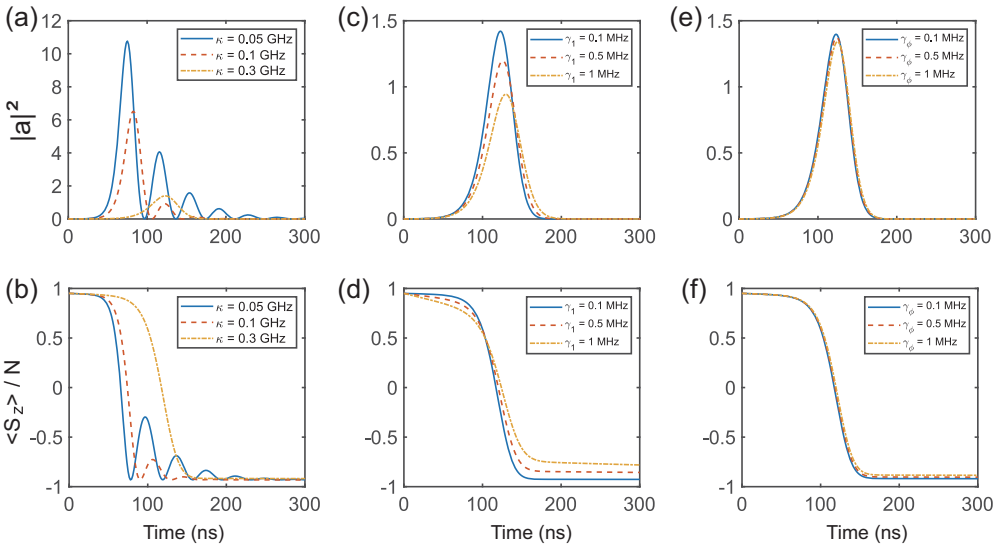

FIG. 6. Dynamics of phonon superradiance for different dissipative processes. Except for the parameters specified in the figure, the remaining parameters are: atom numbers $N = 20$, coupling strength $g_0 = 20\,\mathrm{MHz}$, waveguide leakage rate $\kappa = 0.3\,\mathrm{GHz}$, atomic relaxation rate $\gamma_1 = 0.145\,\mathrm{MHz}$, atomic dephasing rate $\gamma_\phi = 0.125\,\mathrm{MHz}$.

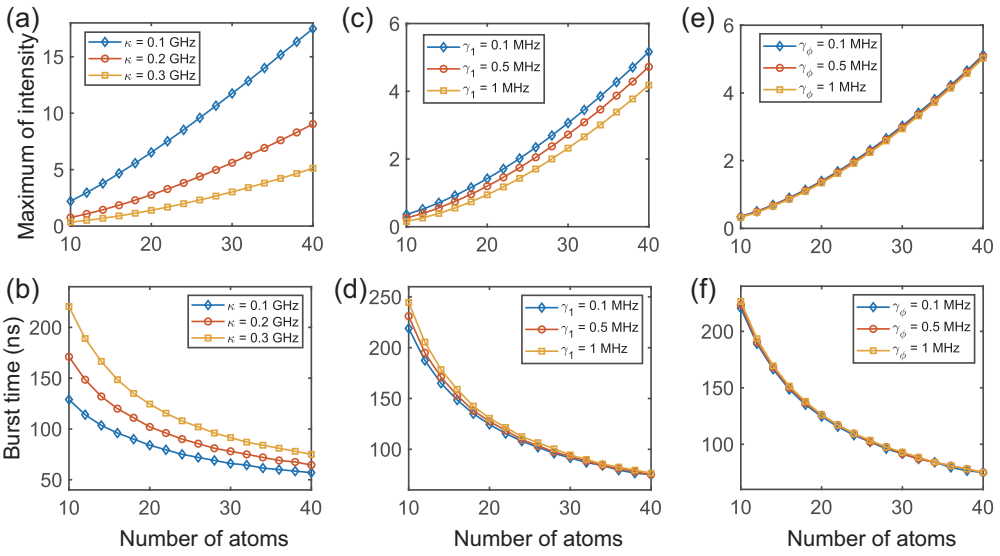

FIG. 7. Scaling laws of phonon superradiance for different dissipative processes. Except for the parameters specified in the figure, the remaining parameters are: atom numbers $N = 20$, coupling strength $g_0 = 20\,\mathrm{MHz}$, waveguide leakage rate $\kappa = 0.3\,\mathrm{GHz}$, atomic relaxation rate $\gamma_1 = 0.145\,\mathrm{MHz}$, atomic dephasing rate $\gamma_\phi = 0.125\,\mathrm{MHz}$.

waveguide case, Rabi oscillations occur between phonons and atomic ensembles, leading to a multipeaked structure of phonon radiation. In contrast, in the fast waveguide case, the emitted phonon field appears as a single-peaked structure, which is characteristic of superradiance. At the same time, the rapid leakage of the waveguide leads to a decrease in the peak intensity of the phonon radiation.

In Figs. 6(c) and 6(d), we show the effect of the atomic relaxation rate on the dynamics of the hybrid system. The relaxation effect plays a significant role in the process of collective decay of atoms and in the phonon radiation processes. This leads to the fact that the atomic ensemble does not decay to the initial ground state and also reduces the peak intensity of phonon superradiance.

In Figs. 6(e) and 6(f), we show the effect of the atomic dephasing rate on phonon superradiance. The results show that the dephasing rate has only a slight effect on the peak intensity of the phonon field and on the polarization of the atomic ensemble. This indicates that this collective dynamics has a coherent behavior and can find potential applications in quantum information processing.

2. Dissipation effects on scaling laws in the small atom regime

Since phonon superradiance is a coherent process of collective atoms, it is of interest to study the effect of dissipation on scaling laws. In Figs. 7(a) and 7(b), we show the effect of waveguide leakage on the scaling law. The results show that the smaller the waveguide leakage, the stronger the peak phonon radiation and the shorter the phonon burst time. As shown in Figs. 7(c) and 7(d), the atomic relaxation shows a similar effect as the waveguide leakage. These results are consistent with expectations. After the pulse driving, the atom ensemble reaches a highly excited state and remains in this excited state for some time. Then the collective atoms decay and a burst of phonons flows into the waveguide. When the atomic relaxation rate or waveguide leakage rate increases, it stimulates the atomic ensembles to decay out of the highly excited state faster.

In Figs. 7(e) and 7(f), we show the effect of the atomic dephasing rate on the scaling laws. The results show that the dephasing rate has only a slight effect on the scaling laws. This is consistent with the effect of the dephasing rate on the dynamics of the hybrid system.

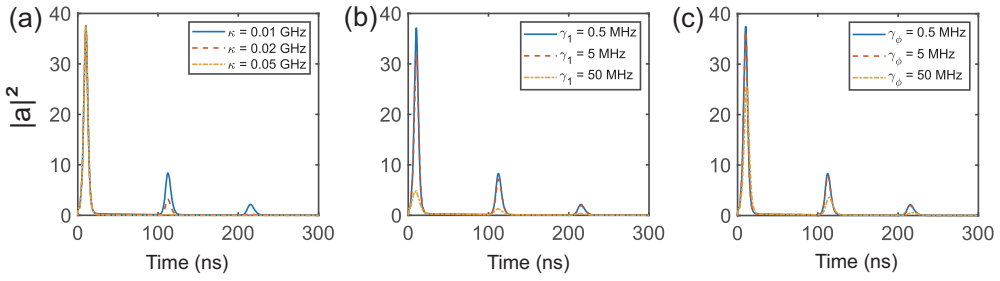

FIG. 8. Collective dynamics for different delay times and dissipation times. Except for the parameters specified in the figure, the remaining parameters are: giant atom numbers $N = 20$, coupling strength $g_0 = 50\,\mathrm{MHz}$, waveguide leakage rate $\kappa = 10\,\mathrm{MHz}$, atomic relaxation rate $\gamma_1 = 0.145\,\mathrm{MHz}$, atomic dephasing rate $\gamma_\phi = 0.125\,\mathrm{MHz}$, delay time $\tau_d = 100\,\mathrm{ns}$.

3. Competing effects between delay times and various dissipation times in the giant atom regime

By numerically solving the equations of motion (6) of the hybrid system in the main text, we give the simulation results of its dynamics in the giant atom regime. During the process of phonon superradiance, on the one hand, the giant atoms emit phonons, and on the other hand, the already emitted phonons are reabsorbed by the giant atoms. The first process is determined by the decay time of the giant atoms and the second by the delay time of the phonon field. These two characteristic times are comparable, so they compete with each other and lead to a change in the phonon superradiance. In Fig. 8, we show the time-delayed dynamics for different dissipation times. The results show that the intensity of the phonon radiation peak decreases as the waveguide leakage rate and the atomic relaxation rate increase. In contrast, the atomic dephasing has little effect on the phonon radiation process.

[1] J. M. Raimond, M. Brune, and S. Haroche, Manipulating quantum entanglement with atoms and photons in a cavity, Rev. Mod. Phys. **73**, 565 (2001).

[2] R. Miller, T. E. Northup, K. M. Birnbaum, A. Boca, A. D. Boozer, and H. J. Kimble, Trapped atoms in cavity QED: Coupling quantized light and matter, J. Phys. B **38**, S551 (2005).

[3] H. J. Kimble, The quantum internet, Nature (London) **453**, 1023 (2008).

[4] R. J. Schoelkopf and S. M. Girvin, Wiring up quantum systems, Nature (London) **451**, 664 (2008).

[5] W. Ge, K. Jacobs, Z. Eldredge, A. V. Gorshkov, and M. Foss-Feig, Distributed quantum metrology with linear networks and separable inputs, Phys. Rev. Lett. **121**, 043604 (2018).

[6] M. V. Gustafsson, T. Aref, A. F. Kockum, M. K. Ekstrom, G. Johansson, and P. Delsing, Propagating phonons coupled to an artificial atom, Science **346**, 207 (2014).

[7] R. Manenti, A. F. Kockum, A. Patterson, T. Behrle, J. Rahamim, G. Tancredi, F. Nori, and P. J. Leek, Circuit quantum acoustodynamics with surface acoustic waves, Nat. Commun. **8**, 975 (2017).

[8] A. Noguchi, R. Yamazaki, Y. Tabuchi, and Y. Nakamura, Qubit-assisted transduction for a detection of surface acoustic waves near the quantum limit, Phys. Rev. Lett. **119**, 180505 (2017).

[9] A. N. Bolgar, J. I. Zotova, D. D. Kirichenko, I. S. Besedin, A. V. Semenov, R. S. Shaikhaidarov, and O. V. Astafiev, Quantum regime of a two-dimensional phonon cavity, Phys. Rev. Lett. **120**, 223603 (2018).

[10] B. A. Moores, L. R. Sletten, J. J. Viennot, and K. W. Lehnert, Cavity quantum acoustic device in the multimode strong coupling regime, Phys. Rev. Lett. **120**, 227701 (2018).

[11] G. Andersson, M. K. Ekstrom, and P. Delsing, Electromagnetically induced acoustic transparency with a superconducting circuit, Phys. Rev. Lett. **124**, 240402 (2020).

[12] A. Bienfait, Y. P. Zhong, H.-S. Chang, M.-H. Chou, C. R. Conner, E. Dumur, J. Grebel, G. A. Peairs, R. G. Povey, K. J. Satzinger, and A. N. Cleland, Quantum erasure using entangled surface acoustic phonons, Phys. Rev. X **10**, 021055 (2020).

[13] A. Frisk Kockum, P. Delsing, and G. Johansson, Designing frequency-dependent relaxation rates and Lamb shifts for a giant artificial atom, Phys. Rev. A **90**, 013837 (2014).

[14] L. Guo, A. L. Grimsmo, A. F. Kockum, M. Pletyukhov, and G. Johansson, Giant acoustic atom: A single quantum system with a deterministic time delay, Phys. Rev. A **95**, 053821 (2017).

[15] L. Guo, A. F. Kockum, F. Marquardt, and G. Johansson, Oscillating bound states for a giant atom, Phys. Rev. Res. **2**, 043014 (2020).

[16] A. F. Kockum, G. Johansson, and F. Nori, Decoherence-free interaction between giant atoms in waveguide quantum electrodynamics, Phys. Rev. Lett. **120**, 140404 (2018).

[17] A. Gonzalez-Tudela, C. Sanchez Munoz, and J. I. Cirac, Engineering and Harnessing giant atoms in high-dimensional baths: A Proposal for implementation with cold atoms, Phys. Rev. Lett. **122**, 203603 (2019).

[18] G. Andersson, B. Suri, L. Guo, T. Aref, and P. Delsing, Nonexponential decay of a giant artificial atom, Nat. Phys. **15**, 1123 (2019).

[19] B. Kannan, M. Ruckriegel, D. Campbell, A. F. Kockum, J. Braumuler, D. Kim, M. Kjaergaard, P. Krantz, A. Melville, B. M. Niedzielski, A. Vepsalainen, R. Winik, J. Yoder, F. Nori, T. P. Orlando, S. Gustavsson, and W. D. Oliver, Waveguide quantum electrodynamics with superconducting artificial giant atoms, Nature (London) **583**, 775 (2020).

[20] L. R. Sletten, B. A. Moores, J. J. Viennot, and K. W. Lehnert, Resolving phonon fock states in a multimode cavity with a double-slit qubit, Phys. Rev. X **9**, 021056 (2019).

[21] A. M. Vadiraj, A. Ask, T. G. McConkey, I. Nsanzineza, C. W. Sandbo Chang, A. F. Kockum, and C. M. Wilson, Engineering the level structure of a giant artificial atom in waveguide quantum electrodynamics, engineering the level structure of a giant artificial atom in waveguide quantum electrodynamics, Phys. Rev. A **103**, 023710 (2021).

[22] X. Wang, T. Liu, A. F. Kockum, H.-R. Li, and F. Nori, Tunable chiral bound states with giant atoms, Phys. Rev. Lett. **126**, 043602 (2021).

[23] L. Du, Y. Zhang, J.-H. Wu, A. F. Kockum, and Y. Li, Giant atoms in a synthetic frequency dimension, Phys. Rev. Lett. **128**, 223602 (2022).

[24] A. C. Santos and R. Bachelard, Generation of maximally entangled long-lived states with giant atoms in a waveguide, Phys. Rev. Lett. **130**, 053601 (2023).

[25] R. H. Dicke, Coherence in spontaneous radiation processes, Phys. Rev. **93**, 99 (1954).

[26] M. Gross, and S. Haroche, Superradiance: an essay on the theory of collective spontaneous emission, Phys. Rep. **93**, 301 (1982).

[27] R. G. DeVoe and R. G. Brewer, Observation of superradiant and subradiant spontaneous emission of two trapped ions, Phys. Rev. Lett. **76**, 2049 (1996).

[28] V. V. Temnov, and U. Woggon, Superradiance and subradiance in an inhomogeneously broadened ensemble of two-level systems coupled to a low-Q cavity, Phys. Rev. Lett. **95**, 243602 (2005).

[29] M. Scheibner, T. Schmidt, L. Worschech, A. Forchel, G. Bacher, T. Passow, and D. Hommel, Superradiance of quantum dots, Nat. Phys. **3**, 106 (2007).

[30] J. A. Mlynek, A. A. Abdumalikov, C. Eichler, and A. Wallraff, Observation of Dicke superradiance for two artificial atoms in a cavity with high decay rate, Nat. Commun. **5**, 5186 (2014).

[31] P. Solano, P. Barberis-Blostein, F. K. Fatemi, L. A. Orozco, and S. L. Rolston, Super-radiance reveals infinite-range dipole interactions through a nanofiber, Nat. Commun. **8**, 1857 (2017).

[32] L. Chen, P. Wang, Z. Meng, L. Huang, H. Cai, D.-W. Wang, S.-Y. Zhu, and J. Zhang, Experimental observation of one-dimensional superradiance lattices in ultracold atoms, Phys. Rev. Lett. **120**, 193601 (2018).

[33] A. Angerer *et al.*, Superradiant emission from colour centres in diamond, Nat. Phys. **14**, 1168 (2018).

[34] Z. Wang, H. Li, W. Feng, X. Song, C. Song, W. Liu, Q. Guo, X. Zhang, H. Dong, D. Zheng, H. Wang, and D.-W. Wang, Controllable switching between superradiant and subradiant states in a 10-qubit superconducting circuit, Phys. Rev. Lett. **124**, 013601 (2020).

[35] X. Gu, A. F. Kockum, A. Miranowicz, Y.-X. Liu, and F. Nori, Microwave photonics with superconducting quantum circuits, Phys. Rep. **718-719**, 1 (2017).

[36] M. Kjaergaard, M. E. Schwartz, J. Braumuller, P. Krantz, J. I.-J. Wang, S. Gustavsson, and W. D. Oliver, Superconducting qubits: Current state of play, Annu. Rev. Condens. Matter Phys. **11**, 369 (2020).

[37] J. Koch, T. M. Yu, J. Gambetta, A. A. Houck, D. I. Schuster, J. Majer, A. Blais, M. H. Devoret, S. M. Girvin, and R. J. Schoelkopf, Charge-insensitive qubit design derived from the Cooper pair box, Phys. Rev. A **76**, 042319 (2007).

[38] P. Y. Wen, K.-T. Lin, A. F. Kockum, B. Suri, H. Ian, J. C. Chen, S. Y. Mao, C. C. Chiu, P. Delsing, F. Nori, G.-D. Lin, and I.-C. Hoi, Large collective lamb shift of two distant superconducting artificial atoms, Phys. Rev. Lett. **123**, 233602 (2019).

[39] B. Julsgaard and K. Molmer, Dynamical evolution of an inverted spin ensemble in a cavity: Inhomogeneous broadening as a stabilizing mechanism, Phys. Rev. A **86**, 063810 (2012).

[40] K. Lalumiere, B. C. Sanders, A. F. van Loo, A. Fedorov, A. Wallraff, and A. Blais, Input-output theory for waveguide QED with an ensemble of inhomogeneous atoms, Phys. Rev. A **88**, 043806 (2013).

[41] N. Lambert, Y. Matsuzaki, K. Kakuyanagi, N. Ishida, S. Saito, and F. Nori, Superradiance with an ensemble of superconducting flux qubits, Phys. Rev. B **94**, 224510 (2016).

[42] K. Kakuyanagi, Y. Matsuzaki, C. Deprez, H. Toida, K. Semba, H. Yamaguchi, W. J. Munro, and S. Saito, Observation of collective coupling between an engineered ensemble of macroscopic artificial atoms and a superconducting resonator, Phys. Rev. Lett. **117**, 210503 (2016).

[43] B. C. Rose, A. M. Tyryshkin, H. Riemann, N. V. Abrosimov, P. Becker, H. J. Pohl, M. L. W. Thewalt, K. M. Itoh, and S. A. Lyon, Coherent Rabi dynamics of a superradiant spin ensemble in a microwave cavity, Phys. Rev. X **7**, 031002 (2017).

[44] Z.-L. Xiang, S. Ashhab, J. Q. You, and F. Nori, Hybrid quantum circuits: Superconducting circuits interacting with other quantum systems, Rev. Mod. Phys. **85**, 623 (2013).

[45] G. Kurizki, P. Bertet, Y. Kubo, K. Molmer, D. Petrosyan, P. Rabl, and J. Schmiedmayer, Quantum technologies with hybrid systems, Proc. Natl. Acad. Sci. USA **112**, 3866 (2015).

[46] A. A. Clerk, K. W. Lehnert, P. Bertet, J. R. Petta and Y. Nakamura, Hybrid quantum systems with circuit quantum electrodynamics, Nat. Phys. **16**, 257 (2020).

[47] J. S. Douglas, H. Habibian, C.-L. Hung, A. Gorshkov, H. J. Kimble, and D. E. Chang, Quantum many-body models with cold atoms coupled to photonic crystals, Nat. Photon **9**, 326 (2015).

[48] H. Pichler, T. Ramos, Andrew J. Daley, and P. Zoller, Quantum optics of chiral spin networks, Phys. Rev. A **91**, 042116 (2015).

[49] H. Pichler, S. Choi, P. Zoller, and M. D. Lukin, Universal photonic quantum computation via time-delayed feedback, Proc. Natl. Acad. Sci. USA **114**, 11362 (2017).

[50] H. Pichler and P. Zoller, Photonic Circuits with Time Delays and Quantum Feedback, Phys. Rev. Lett. **116**, 093601 (2016).

[51] R. Jones, G. Buonaiuto, B. Lang, I. Lesanovsky, and B. Olmos, Collectively enhanced chiral photon emission from an atomic array near a nanofiber, Phys. Rev. Lett. **124**, 093601 (2020).

[52] J. G. Bohnet *et al.*, A steady-state superradiant laser with less than one intracavity photon, Nature (London) **484**, 78 (2012).

[53] M. A. Norcia, M. N. Winchester, J. R. K. Cline, and J. K. Thompson, Superradiance on the millihertz linewidth strontium clock transition, Sci. Adv. **2**, e1601231 (2016).

[54] S. D. Bennett,N. Y. Yao, J. Otterbach, P. Zoller, P. Rabl, and M. D. Lukin, Phonon-induced spin–spin interactions in diamond nanostructures: Application to spin squeezing, Phys. Rev. Lett. **110**, 156402 (2013).

[55] R. Bianchetti, S. Filipp, M. Baur, J. M. Fink, M. Goppl, P. J. Leek, L. Steffen, A. Blais, and A. Wallraff, Dynamics of dispersive single-qubit readout in circuit quantum electrodynamics, Phys. Rev. A **80**, 043840 (2009).